



Effect of copper nanoparticles on physico-chemical properties of chitosan and gelatin-based scaffold developed for skin tissue engineering application

Shikha Kumari¹ · Bhisam Narayan Singh¹ · Pradeep Srivastava¹

Received: 16 October 2018 / Accepted: 8 February 2019 / Published online: 21 February 2019
© King Abdulaziz City for Science and Technology 2019

Abstract

Development of new and effective scaffold continues to be an area of intense research in skin tissue engineering. The objective of this study was to study the effect of copper nanoparticles over physico-chemical properties of the chitosan and gelatin composite scaffolds for skin tissue engineering. The copper-doped scaffolds were prepared using freeze-drying method. Chitosan and gelatin were taken in varied composition with 0.01%, 0.02%, and 0.03% Cu nanoparticles. The physico-chemical properties of the copper nanoparticles and the scaffolds were analyzed using Fourier transform infrared spectroscopy (FTIR), X-ray diffraction (XRD), scanning electron microscopy (SEM), and transmission electron microscopy. Porosity of the scaffolds was measured by liquid displacement method and hemocompatibility was tested using goat blood. SEM micrographs of the scaffolds displayed the interconnected pores which ranged between 25 and 40 μm . This average pore size was later enhanced to 95 μm after the addition of copper nanoparticles. Cell viability assay was performed to ensure the growth and proliferation of the skin cells over the scaffolds. FTIR, EDS, and XRD analysis of scaffolds confirmed the presence of copper in the chitosan-based scaffolds. Porosity measurement showed the interconnectivity between pores which ranged between 65 and 88% as required for skin tissue engineering application. The degradation study of the scaffolds was done which depicted that, after the addition of copper nanoparticles with 0.03%, degradation rate was decreased. SEM and cytocompatibility assay on all scaffolds showed the cell adhesion and proliferation on the scaffolds which was not affected after addition of copper nanoparticles. Oxidative stress evaluation was done to study the effect of copper nanoparticles on the cells which showed that there was no such production of ROS in the scaffolds. Hence, scaffolds prepared after doping of copper nanoparticles show suitable physico-chemical and biological properties for skin tissue engineering application.

Keywords Skin tissue engineering · Copper nanoparticles · Chitosan · Gelatin · Wound healing · Scaffold · Nanocomposite scaffold · Mechanical property

Introduction

There have been significant developments in the past decades, in the field of skin tissue engineering. The skin tissue engineering approach aims to restore normal skin by fabricating three-dimensional scaffolds analogous to the extracellular matrix which guide cell adhesion and their migration to the wound site to speed up the healing process. Several tissue-engineered constructs have been developed in past

years for the replacement of damaged skin. However, certain shortcomings have always restricted the application of available substitutes. Issues like scar formation and poor tissue integration have always enforced the researchers to focus on the development of skin substitutes that play an active role in wound healing (Yildirimer et al. 2012). A skin substitute for wound healing requires porous degradable materials called as scaffolds which help in repairing and regeneration of damaged and injured tissues. The scaffold material should promote cell differentiation, act as a barrier to physical environment, absorb wound exudates, allow nutrient and gaseous exchange, improve the healing process, promote cell adhesion, reduce the bacterial load, and promote proliferation of cells (Chhabra et al. 2016). An ideal scaffold for tissue regeneration should be biocompatible, biodegradable,

✉ Pradeep Srivastava
pksrivastava.bce@itbhu.ac.in

¹ School of Biochemical Engineering, Indian Institute of Technology, Varanasi 221005, India

bioactive, porous, and mechanically compatible. Physical attributes can be imparted to them by the addition of metallic nanoparticles into it. Metal nanoparticles like Zn, Au, and Ag have been used in past for studying the anti-inflammatory property, antibacterial properties, and mechanical strength of the scaffold. However, metals like Cu are still finding their way in the scaffold preparation.

Copper is a crucial trace element, and it plays a key role in angiogenesis and in expression and stabilization of extracellular skin proteins. It also exhibits broad biocidal properties (Borkow et al. 2010). Copper is mobilized to injured sites to enhance host defense and early wound-healing mechanisms (Zinc et al. 2013).

The proangiogenic property of copper is exhaustively documented (Hu 1998; Sen et al. 2002; Martin et al. 2005; Gérard et al. 2010). In addition, it is observed that copper induces vascular endothelial growth factor in wounds (Sen et al. 2002) possibly by stabilizing hypoxia-inducible factor-1 α (Martin et al. 2005). There are no data on the consequences of copper deficiency per se on wound healing except for a case report (Liusuwan et al. 2008). The advancement in nanotechnology and cell therapy has opened new ways for making smart skin substitutes for accelerated wound healing. Study on copper nanoparticles composite hydrogels was done showing the efficacy of chitosan-based copper nanocomposite in wound-healing phenomenon (Gopal et al. 2014). Later, in 2015, study was conducted, wherein copper nanoparticles in chitosan scaffolds were shown to promote bone regeneration (D'Mello et al. 2015).

Understanding the merits of copper in metal, herein, we have hypothesized that incorporation of copper to scaffold would aid the wound-healing potential of scaffolds by enhancing the VEGFs and provide antibacterial property to skin substitutes. In the present novel study, nanocomposite scaffold of copper and chitosan and gelatin has been made for skin tissue engineering application. Gelatin has been chosen because of associated advantages such as non-antigenicity, biodegradability, commercial availability, and biocompatibility. Chitosan is also biodegradable and biocompatible in nature and, therefore, suitable for skin tissue engineering application (Ueno et al. 2001; Azad 2004). Several studies have been done where nanocomposite scaffolds were used for alveolar tissue engineering application also using chitosan and gelatin scaffolds impregnated with nanobioglass (Peter et al. 2010).

Materials

Chitosan, gelatin, fetal bovine serum (FBS), dispase, Dulbecco's modified eagle's medium (DMEM), glacial acetic acid, antibiotics, collagenase-I, glutamine solution, and DCFDA-Cellular Reactive Oxygen Species Detection

Assay Kit were purchased from HiMedia (Mumbai, India). Copper sulfate, sodium hydroxide, Trypsin-EDTA, Bovine Serum Albumin, and Bradford's reagent was purchased from Merck, India. L-Ascorbic acid and Starch were purchased from Sigma-Aldrich, US. Cell Viability Assay Kit *Green/Red Dual Fluorescence* was purchased from AAT Bioquest®. All the material used was of reagent grade. Distilled water and Milli-Q water were used for copper nanoparticle synthesis and cell culture experiments, respectively.

Methods

Synthesis of Cu nanoparticles

The copper nanoparticles were synthesized using a chemical reduction approach in which copper(II) sulfate pentahydrate had been used as a precursor salt, while starch was also added as capping agent. First, 0.1 M of 100 mL copper(II) sulfate pentahydrate solution was added into 1.2% of 240 mL of starch solution along with vigorous stirring for 30 min followed by the second step in which 0.2 M of 100 mL ascorbic acid solution was added into the previous solution under constant stirring. Subsequently, 1 M of 60 mL sodium hydroxide solution was added to the above-prepared solution followed with undisturbed stirring and heating at 80 °C for 1.30 h. A color change was observed from yellow to ocher color after it (Khan et al. 2016). Thereafter, the reaction got completed and the solution was taken up from the heat and it was allowed to settle overnight. After 24 h, the supernatant was vigilantly discarded and the precipitate was separated from that solution by centrifugation at 10,000 rpm. Then, the precipitate was washed using ethanol and deionized water for 3–4 times to take out the excessive starch bound with the nanoparticles. Ocher color precipitates obtained were dried in a vacuum oven at room temperature. After drying, the nanoparticles were stored for further analysis.

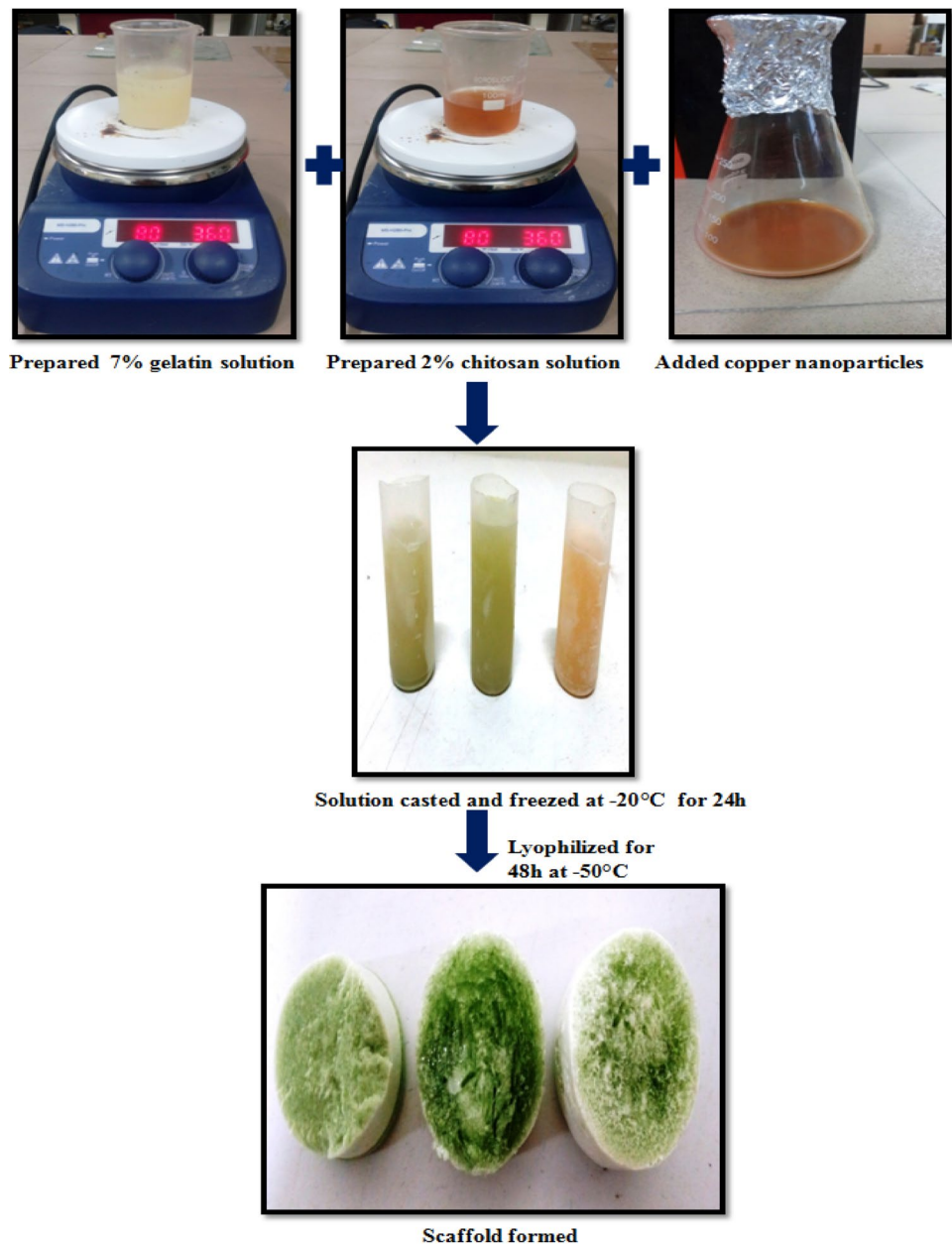
Fabrication of copper nanoparticle-loaded porous scaffold

Chitosan was dissolved in 1% of 1 M CH₃COOH (acetic acid) aqueous solution to form a 2% polymer solution with constant rapid stirring at 37 °C temperature. Thereafter, 7% polymer solution of gelatin was made by dissolving 7 gm of gelatin in 100 mL of distilled water at constant stirring. Three samples were made with different compositions of chitosan and gelatin. These samples were poured into DPS tubes and frozen at –20 °C for overnight. After 24 h, the frozen polymer blend solutions were lyophilized at –50 °C temperature using labconco lyophilizer. Table 1 shows the composition used for preparing the scaffolds without copper nanoparticles and with copper nanoparticles.

Table 1 Composition of scaffolds prepared

Sample no.	Chitosan (%age)	Gelatin (%age)	Copper nanoparticles (%)
F 1	50	50	N/A
F 2	25	75	N/A
F 3	75	25	N/A
F 4	50	50	0.01
F 5	25	25	0.02
F 6	75	75	0.03

The copper-chitosan scaffolds were prepared by adding slowly blend of 2% w/v chitosan solution and 7% w/v solution of gelatin to 50 mL 0.01% copper, then 0.02%, and finally 0.03% copper solution. The mixture was vortexed for 5 m for homogeneity, and was poured into DPS tubes and further incubated overnight at -20°C and later freeze-dried to completely remove the solvent. Addition of chitosan solution to the copper solution led to the color change of chitosan and gelatin solution to greenish color. Figure 1 shows the preparation of the scaffolds with copper nanoparticles.

Fig. 1 Preparation of chitosan- and gelatin-based scaffolds with copper nanoparticles

Characterization of copper nanoparticles

Scanning electron microscopy (SEM) and energy-dispersive X-ray (EDX)

Surface morphology of the synthesized nanoparticles was examined by scanning electron microscopy (SEM, ZEISS-EVO18) combined with an energy-dispersive X-ray spectrometer (EDX) (6490 LA). Sample preparation for SEM was done in powdered form, and since the nanoparticles were already dried, and, therefore, the same powder was used for analysis. Only a small pinch of nanoparticles powder was dispersed onto a double-sided adhesive carbon conductive tape and it was coated using golden sputter coating via ion sputtering device (JFC 1500). This was placed on the sample holder to allow the beam to fall on its surface.

EDX was carried out at an acceleration voltage of 20.0 kV. The same sample of SEM was used to study the elemental composition both in normalized atomic% concentration as well as in normalized weight% concentration.

High-resolution scanning electron microscopy (HRSEM)

High-resolution scanning electron microscopy (HRSEM) was done to observe the nanoparticle size and morphology at a higher resolution using HRSEM FEI NovananoSEM 450 instrument. Nanoparticle powder was first dispersed in 5 mL ethanol and 5 mL water in 1:1 ratio after that this solution was sonicated for 1–2 h to avoid the agglomeration of the nanoparticles. After proper separation of particles, 2 μ L of the suspension was taken on a platinum film and it was allowed to dry at room temperature. Once the suspension was dry, HRSEM characterization was done.

Transmission electron microscopy (TEM)

Transmission electron microscopy was done to characterize the size, shape, and morphology of synthesized copper nanoparticles using FEI-TECNAI G²20 TWIN instrument. Sample preparation for TEM was quite sensitive process. Since the nanoparticles were in powdered form, therefore, first, a small tinge of powdered nanoparticles was immersed in ethanol which was used as a solvent. Furthermore, this solution was sonicated for 20–30 min using ultrasonicator to ensure the proper dispersion of the nanoparticles. Once the suspension was prepared, after that, 2–5 μ L of this suspension was poured onto the grid towards the mesh side, and it was properly smeared and allowed to dry at room temperature.

X-ray diffraction (XRD)

XRD analysis of prepared copper nanoparticles was performed using Rigaku-MiniFlex 600 diffractometer that was operated at 40 kV and 30 mA with Cu Ka radiation (1.54 Å) as a source. The sampling time was 0.5 s and measurement temperature was 25 °C. The scanning range of 2θ was between 20 and 90 °C. Sample preparation for XRD was easy as the nanoparticles were synthesized in a powdered form. The nanoparticles powder was placed on top of an aluminum slide and it was ensured that the powdered nanoparticles were spread out properly to cover up the specified area. Mean size of nanoparticles was measured from the broadening of the diffraction peaks. According to the JCPDS database, these peaks indicated the intensive reflections. Determination of the nanoparticles size from XRD diffraction pattern was done using the Scherrer equation:

$$D = \frac{K\lambda}{\beta \cos \theta}, \quad (1)$$

where: (Karp et al. 2003) K = Scherrer constant (shape factor, its value is 0.9), λ = X-ray wavelength ($\lambda = 0.154$ nm), β = line broadening at half the maximum intensity (FWHM) in radians, θ = Bragg angle (the position of the diffraction peak maximum), and d = average dimension of crystallites in nanometers.

Fourier transform infrared spectroscopy was done to examine the functional groups which present and it was recorded using SHIMADZU-IR Affinity-1S FTIR spectrometer. For sample preparation of FTIR, solid KBr powder was allowed to dry for 2 h in hot air oven. Then, afterwards, small amount of sample was ground with KBr and the pellet was prepared by the PCi hydraulic press dye. The pelleted sample was analyzed with FTIR spectrometer to obtain the corresponding peaks for Cu nanoparticles.

Morphological analysis of scaffold

Scanning electron microscopy

For SEM analysis, samples were obtained by cutting a section from the prepared scaffolds. Gold sputter coating was done on the sample's surface, and then, sample was placed on aluminum stubs. The pore size of control and composite scaffolds was calculated using the ImageJ software. To prepare the samples of cell-embedded scaffolds for SEM analysis, fixation and dehydration of cells were carried out with 1% glutaraldehyde solution and dehydration using the series of ethanol aqueous solutions. The ethanol concentration was consecutively increased from 30 to 70% and finally to 99.99% weight.

Structural and functional analysis

X-ray diffraction

The phase analysis of chitosan–gelatin blend scaffolds and chitosan, gelatin, and copper nanoparticles' composite scaffolds was analyzed by X-ray diffractometer and Rigaku-MiniFlex 600 using Cu K α radiation in a step-scan mode in the 2θ range of 10° – 50° .

Fourier transform infrared spectroscopy (FTIR)

Fourier transform infrared spectroscopy (FTIR) was performed in IR Affinity-1S FTIR spectrophotometer, SHIMADZU to know the structural information of the Chitosan and gelatin blend scaffolds as well as chitosan, gelatin, and copper nanoparticles incorporated composite scaffolds. It helped in the identification of different functional groups of chitosan, gelatin, and other components in scaffold, in range 500 – 4500 cm^{-1} .

Porosity measurement

Liquid displacement method was applied for measuring porosity of the scaffolds (Guan et al. 2005). Absolute ethanol of known volume (V_1) with density ρ was used as displacement liquid, because it can easily penetrate the scaffolds and would not induce shrinking or swelling as a non-solvent of chitosan and gelatin. The scaffold samples F1, F2, F3, F4, F5, and F6 of $2\text{ cm} \times 2\text{ cm}$ were dipped in ethanol for 5 min, and then, the ethanol impregnated scaffold's weight (V_2) was measured. After that, scaffolds were removed and the residual ethanol volume was also recorded (V_3). With the above information, the porosity of scaffolds was calculated by the following equation:

$$\text{Porosity 'P'} = (V_1 - V_3)/(V_2 - V_3). \quad (2)$$

Hemocompatibility test

Hemocompatibility test was performed of the scaffold samples (Kaur and Thirugnanam 2016). Samples were kept in 10 mL of fresh physiological saline for 30 min duration. After that, 1 mg/mL of potassium citrate solution was added to the goat blood and it was diluted (v/v) in 4:5 ratios with physiological saline. Thereafter, 0.2 mL of diluted blood was added to each scaffold sample and they were incubated at room temperature for 1 h. For positive control, blood was added to distilled water, and for negative control; blood was added to physiological saline. After 1 h, samples were centrifuged at 1000 rpm for 10 min and the absorbance (OD) was measured from the supernatant liquid at 545 nm. The percentage hemolysis was calculated using the following equation:

$$\% \text{ Hemolysis} = (\text{OD}_{\text{test}} - \text{OD}_{\text{negative}} \times 100)/(\text{OD}_{\text{positive}} - \text{OD}_{\text{negative}}). \quad (3)$$

Biodegradability test

In vitro degradation studies were performed for the scaffold samples to determine the weight loss. Dry weight of samples was taken (W_i), and then, they were soaked in PBS for 4 weeks at a constant temperature environment at 37°C . The PBS was not changed during the experiment. Samples were withdrawn at regular time duration and dried at 40°C for 4 days, and their final weights (W_f) were measured. Degradation rates were determined from the weight of residual scaffolds and it was expressed as a percentage of the original weight:

$$\% \text{ Degradation} = (W_i - W_f \times 100)/W_i. \quad (4)$$

In vitro cell study

MTT assay

Cell viability and functional activity were calculated using 5-dimethylthiazol-2-yl-2,5-diphenyltetrazolium bromide (MTT) assay, which measures the mitochondrial dehydrogenase activity of viable cells spectrophotometrically. Cell-seeded scaffold was incubated in a humidified environment 37°C under 5% CO_2 for 3rd, 5th, and 7th day, respectively. Briefly, 20 μL of MTT solution (5 mg/mL) was added to the cell suspension (96-well plate) followed by incubation for 4 h. After that, whole medium was taken out, and the wells were substituted with 200 μL of DMSO and again kept in incubator for 4 h. Thereafter, for 4 h, the absorbance was recorded using microplate reader (2030 multilabel reader victor X3, Perkin Elmer, USA) at a wavelength of 595 nm.

Evaluation of oxidative stress

Cell-seeded scaffolds were treated with dichlorofluorescein diacetate (DCFH-DA) to estimate the levels of intracellular reactive oxygen species produced. 2 μL of 20 μM DCFH-DA dye was added into each well-containing the cell-seeded scaffolds (Moore and rapid 1990). Thereafter, after 30 min of incubation period at 37°C and 5% CO_2 , the cells in each sample were extracted and analyzed using phase contrast microscopy.

Live and dead assay for cell viability assessment

Dual fluorescent staining (DFS) was done using calcein acetoxy methyl (CAM) ester and ethidium homodimer-1 (EHD) to evaluate cell viability in the scaffolds. It labels the intracellular esterase activity and plasma membrane integrity, respectively, giving green and red fluorescence of calcein

and EHD which is easily detectable in fluorescence microscopy (Lee et al. 2012). The solution of EHD (6 μM) and CAM (1 μM) was mixed with cell suspensions to stain the cells in scaffolds (Kummrow et al. 2013).

Morphological analysis

After seeding the cells onto the scaffold, scaffolds were incubated at 37 °C and in 5% CO₂ environment. Viable cell counting was done using hemocytometer on every third day by detaching the cells with 0.25% trypsin/EDTA treatment to analyze the cell growth. These cell-seeded scaffolds were further washed using PBS, and then, they were fixed with 2.5% glutaraldehyde. After fixation of cells onto scaffold, the scaffolds were observed under the phase contrast microscope and also SEM was done for morphological evaluation of the attached cells onto the scaffolds.

Results and discussion

Characterization

Morphological analysis of copper nanoparticles with EDX

SEM was done to analyze the surface morphology of the nanoparticles synthesized. Figure 2a shows the clusters of nanoparticles formed because of the agglomeration occurred in free state of the nanoparticles. It showed the presence of heterogeneous sizes of particles formed capped with starch, whereas EDS spectra were helpful in determining the elemental composition of the synthesized nanoparticles. Figure 2a indicates the presence of Cu, while some traces of O and C were also found which were due to the application of starch as stabilizer in the experiment. Peaks found at binding

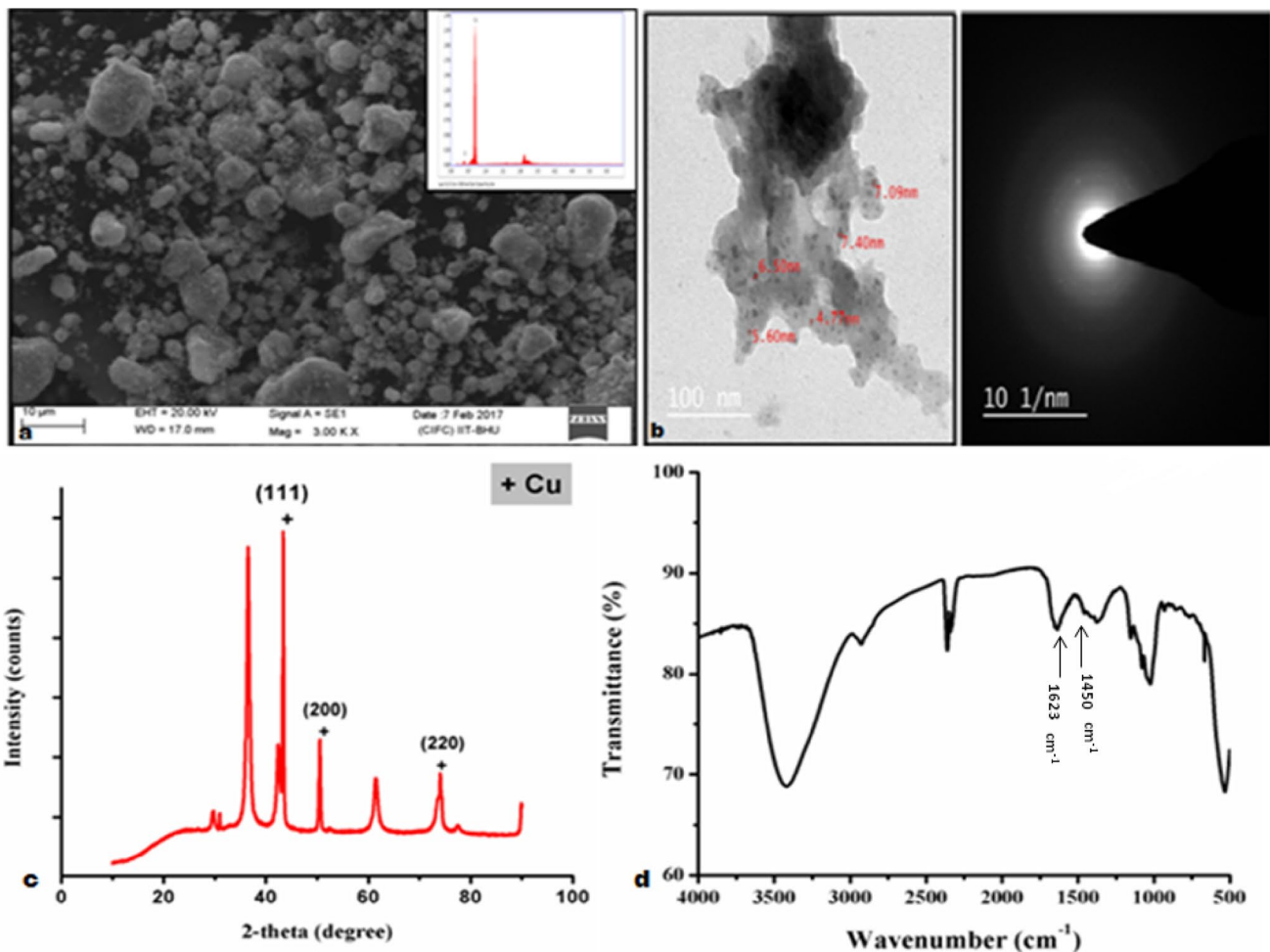


Fig. 2 **a** SEM and EDX micrograph of synthesized nanoparticles and **b** transmission electron microscopic image of copper nanoparticles synthesized of different sizes ranging between 4 and 10 nm and its

diffraction micrograph, **c** XRD image of copper nanoparticles synthesized, and **d** Fourier transform Infrared Spectroscopy graph of copper nanoparticles

energies of 0.98, 8.09, and 8.99 keV confirmed the existence of copper (Karp et al. 2003).

Transmission electron microscopy analysis of copper nanoparticles

SEM defines only the surface morphology of the nanoparticles, and hence, it was important to do the TEM analysis to find the internal composition. Figure 2b shows TEM of nanoparticles synthesized, the average size of nanoparticles found from this analysis is 5.31 nm, and the particles are very well dispersed. It is also clear from TEM that nanoparticles formed are very small in size (Sarkar 2013). Diffraction pattern of TEM for copper nanoparticles is shown in Fig. 2b. As the nanoparticles are very small in size, therefore, only certain dots are visible in it which confirms the amorphous structure of copper nanoparticles synthesized.

Functional and structural analyses of copper nanoparticles

FTIR analysis was done for the nanoparticles to obtain the supplementary information about the nature of nanoparticles. Figure 2d shows the FTIR spectra of copper nanoparticles synthesized. It was done to observe the structural modifications occurred due to cross linking. FTIR spectra of copper nanoparticles showed that the nanoparticles were surrounded by various organic molecules like carboxylic acid, alcohols, ketones, and aldehydes. Broadband that was observed around 616 cm^{-1} depicts the stretching frequency of OH group that was present on the surface of the copper nanoparticles. Other than that peaks observed at 3373 cm^{-1} , 1635 cm^{-1} , 1516 cm^{-1} , 1376 cm^{-1} , 1198 cm^{-1} correspond to O–H-stretching H-bonded alcohols and phenols, and carbonyl stretching and N–H bend primary amines correspond to C–N stretching of the aromatic amino group and C–O-stretching alcohols, ethers, respectively. Peaks at 1623 cm^{-1} and 1450 cm^{-1} correspond to copper nanoparticles (Betancourt-Galindo et al. 2014).

XRD (X-ray diffraction) analysis

XRD analysis was done to analyze the crystal structure and size of the copper nanoparticles. Figure 2c shows the XRD pattern of synthesized nanoparticles. Peaks observed at 2θ values of 43.33° , 50.45° , and 74.10° correspond to h , k , and l values 111, 200, and 220 planes of metallic Cu. It was confirmed by JCPDS card no. 04-0836 for the standard spectrum face centered cubic metallic Cu. The mean size of the Cu nanoparticles calculated from the major diffractions peaks using the Scherrer formula is about 25.318 nm, respectively. Broadening of peak in the XRD pattern shows the presence of small nanoparticles (Yang et al. 2001).

Physical evaluation of the scaffolds

The prepared scaffolds appeared as spongy materials. These scaffolds were brownish white in color. The brown color may be associated with the color of the chitosan, whereas the whitish tinge is associated with the gelatin. An increase in the chitosan proportion within the scaffolds resulted in the increase in the brownish touch. More firmness and strength was added to the scaffolds by addition of gelatin to the chitosan solution in varied proportion. The color of the scaffolds changed from brownish white to greenish white after the addition of copper nanoparticles into the solution in different concentration. It was seen that the stiffness and firmness of the scaffold gradually increased in 1:1 and 1:2 ratio after the addition of copper nanoparticles into it.

Morphology of porous scaffold (SEM image and EDX graph)

The morphological characteristics of the scaffolds were determined by SEM. It also helped in determining the appropriate pore-size distribution which is required for the wound-healing application. These images show that the average pore size of the scaffolds is $35\text{ }\mu\text{m}$ which is quite good for the skin cell infiltration (Yannas 1989). Large surface area of the obtained scaffolds is clear by the SEM images. SEM images of porous scaffolds revealed the interconnectivity of the porous structure, and it also exposed the smooth and homogenous pore walls surface. Figure 3 shows the SEM images of the scaffolds of different compositions of chitosan/gelatin and also after addition of copper nanoparticles. Average pore size for the scaffolds formed after incorporation of copper nanoparticles is about $71\text{ }\mu\text{m}$ which again proves to provide a better strength to the scaffold and also to the cells. It is also proved that fabrication technique affects the pore-size distribution and structure of scaffolds. Hence, it can be said that freeze-drying technique proved to be a beneficial asset in obtaining good pore size and interconnectivity of pores (Hilmi et al. 2013).

Energy-dispersive X-ray analysis of chitosan–gelatin–copper nanoparticle scaffold

EDX spectra of chitosan–gelatin–copper nanoparticles shown in Fig. 3d–f indicated the presence of copper nanoparticles which were incorporated in these scaffolds. Binding energy peaks at 8.03 keV and 8.9 keV confirm copper presence in metallic state. Another peak of copper at 0.83 keV also shows the presence of copper which shows cuprite presence. Other peaks at 0.32 keV and 0.61 keV represented the

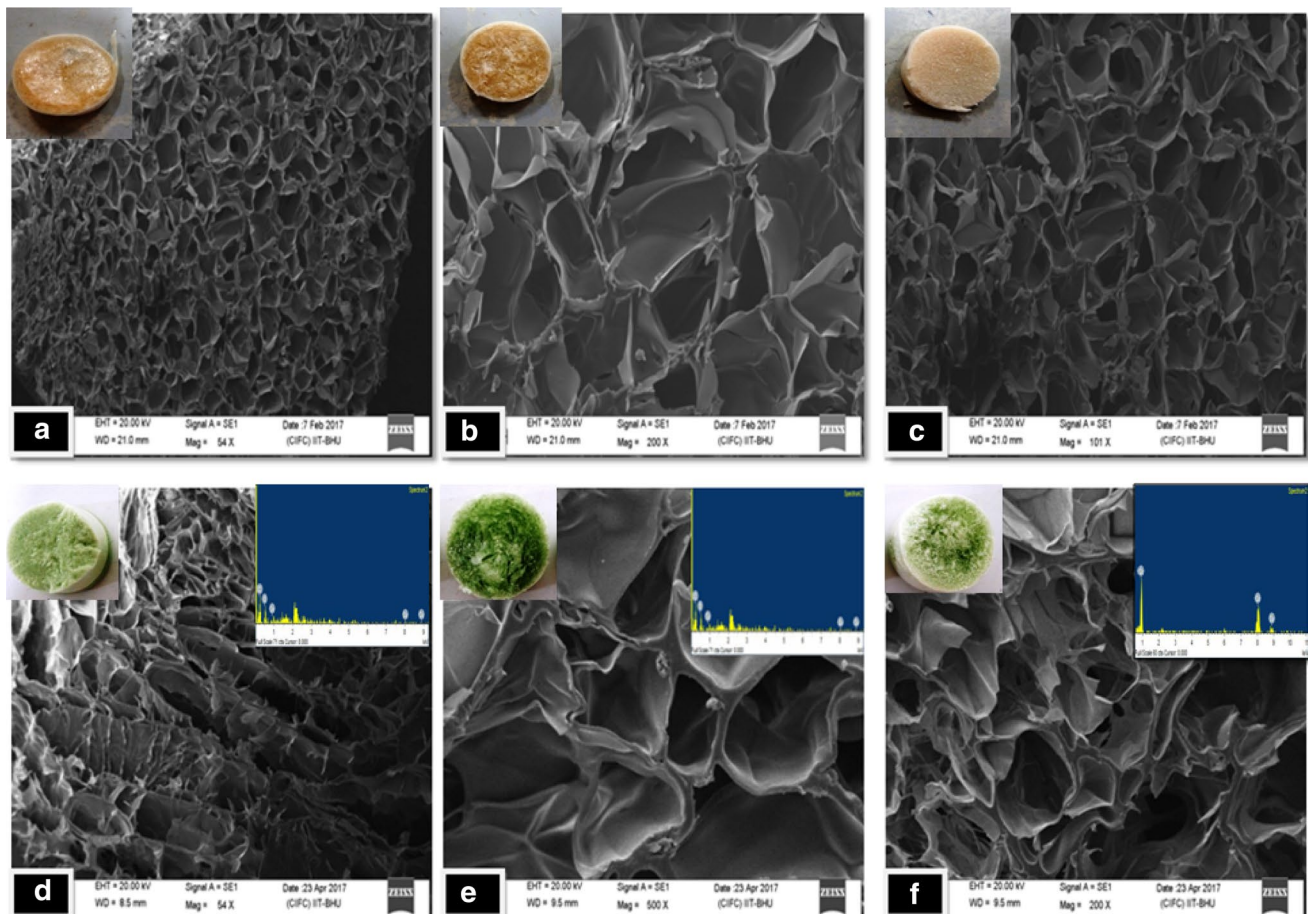


Fig. 3 SEM micrographs of scaffold without copper nanoparticles: **a** F1, **b** F2, and **c** F3, and with copper nanoparticles, **d** F4, **e** F5, and **f** F6 with their physical morphology

presence of C and O, respectively, which shows the presence of carbon stabilizers and certain impurity.

FTIR analysis of chitosan–gelatin composite scaffold and chitosan–gelatin copper nanocomposite scaffold

FTIR analysis was done for the scaffolds which show the functional groups present in the scaffold's component and also the chemical interaction between the functional groups. Cross linking was observed in the structures which showed different modifications in the structure, and, therefore, various bands and peaks were observed. Figure 4 shows the FTIR spectra for scaffolds prepared without copper nanoparticles and with nanoparticles. The FTIR spectra of all the samples showed a broadband around 3425 cm^{-1} and a weak peak at 2900 cm^{-1} which corresponds to CH_2 and OH group. While the band at 1640 cm^{-1} and peak at 1594 cm^{-1} depicts the existence of $\text{C}=\text{O}$ group of acetylated amide and amine groups (Xu et al. 2012). All the three blend samples F1, F2, and F3 consist of the same functional groups, and,

therefore, all their FTIR spectra exhibited bands at 1640 , 1540 , and 1240 cm^{-1} , while, that in F4, F5, and F6 weak peak at 1623 cm^{-1} is observed which is exhibited by copper nanoparticles. In addition, sharp bend can be observed at 1260 cm^{-1} which corresponds to copper interaction with chitosan and gelatin blend.

X-ray diffraction analysis

X-ray diffraction pattern of various scaffolds is shown in Fig. 4 which indicates different peaks corresponding to chitosan and gelatin blend and also chitosan–gelatin copper nanocomposite. The peak bend at approximately 20.53 keV is quite prominent in all the six plots depicting the presence of chitosan. It corresponds to lattice plane 211. This bend is increasing for quite long which represents the blend formed with gelatin. Gelatin is depicted here in the plot by the broad bend at 19.37 keV which is because of combination of gelatin and chitosan (Zhuang et al. 2015). Other than that one more diffraction peak at 2θ around 19.37 keV is prominent in F4, F5, and F6, which corresponds to copper

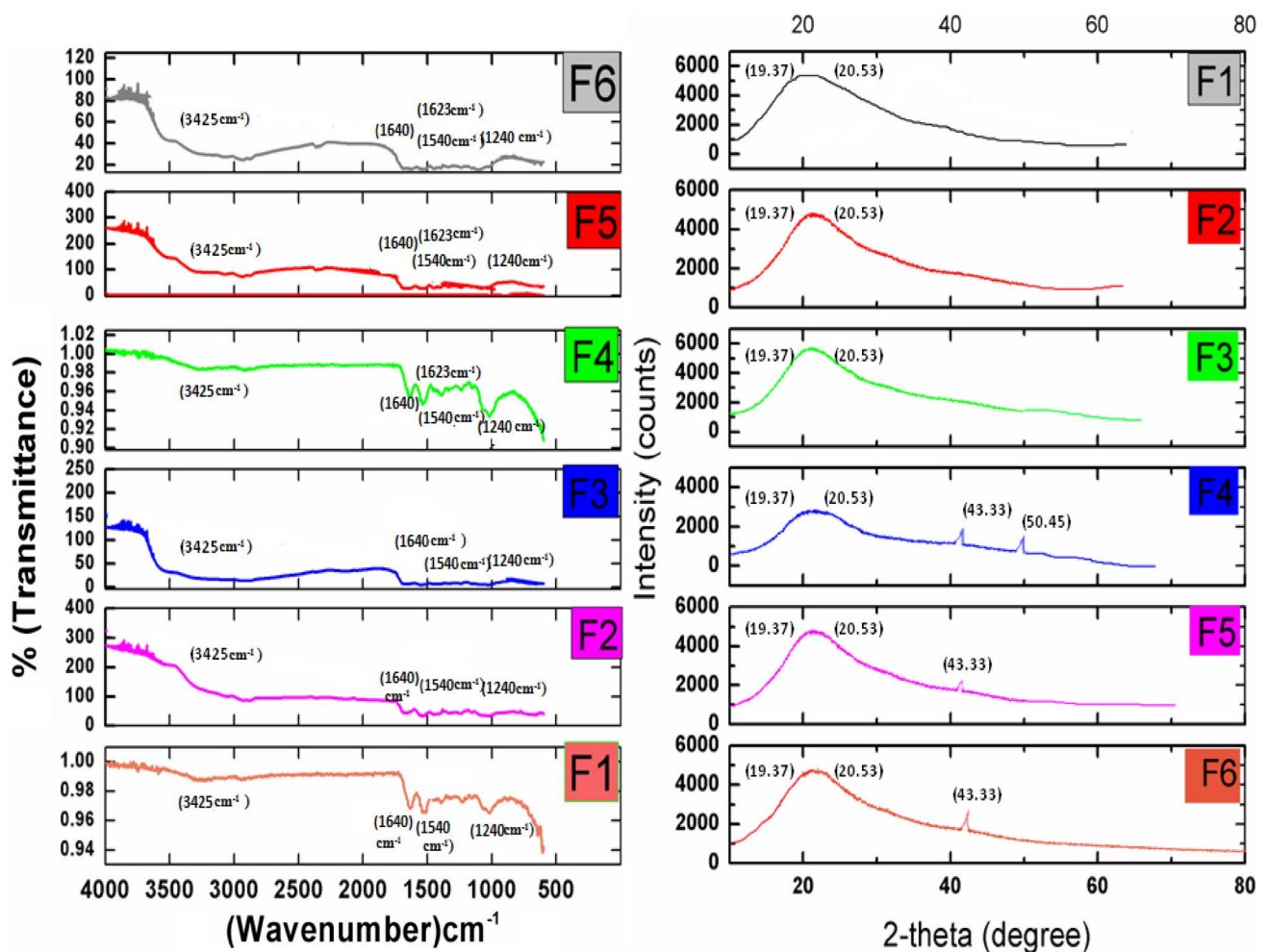


Fig. 4 FTIR and XRD graphs of the scaffolds without copper nanoparticles: **a** F1, **b** F2, and **c** F3, and with copper nanoparticles: **d** F4, **e** F5, and **f** F6

nanoparticles present in the scaffolds. Another peak is observed in F4 at 50.45 keV which again corresponds to copper nanoparticles. The sharpness of this peak attributes a high degree of crystallinity.

Porosity

Porosity of the scaffolds is depicted in Fig. 5, which shows that, with increase in chitosan concentration, the porosity of the scaffolds is reducing. It is also clear from this graph that the scaffold with 0.1% copper nanoparticles and with 1:1 ratio of chitosan and gelatin is having the highest porosity. This means that the copper nanoparticles embedded scaffold with 1:1 ratio of chitosan and gelatin is best suitable for cell proliferation and their attachment. Simultaneous addition of copper nanoparticles into the scaffold resulted into decreased porosity. This might have occurred due to the aggregation of the nanoparticles over the scaffold's surface and would have increased the compactness of the scaffold

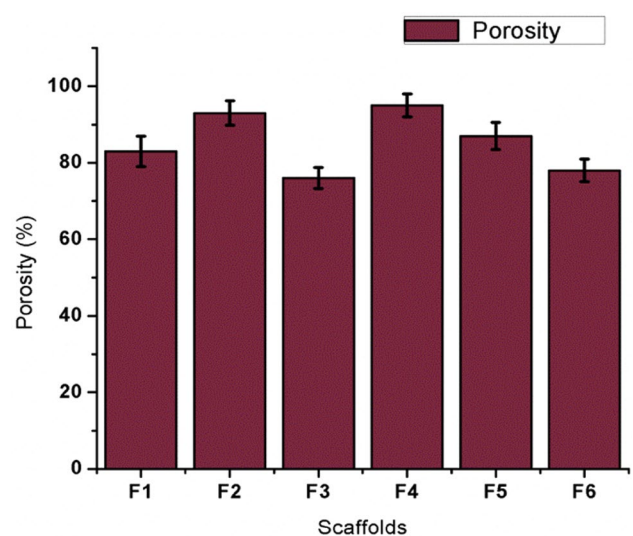


Fig. 5 Porosity of the scaffolds without copper nanoparticles and with copper nanoparticles

which ultimately would have the loss of interconnectivity of the pores. Uniform pore distribution can also be seen in the control scaffolds where highest porosity is found in the chitosan and gelatin scaffold with 2:1 ratio, i.e., with increase in chitosan concentration, porosity of scaffolds has also increased.

This may be associated with the water uptake rate by the scaffold, because it generally depend upon the size and amount of pores. This may be an important aspect for a scaffold developed specifically for wound-healing application, because moist environment is essential for a wound to heal completely.

Table 2 Hemocompatibility study of the scaffolds with and without copper nanoparticles

Sample no.	% Hemolysis
OD _{positive}	0.761
OD _{negative}	0.079
F1	1.32
F2	1.76
F3	2.78
F4	1.47
F5	2.35
F6	3.22

Hemocompatibility study

Table 2 shows the hemocompatibility study of the scaffolds which were made from different composition of chitosan and gelatin. As per the ASTM standard, the hemocompatibility should be lesser than 5 and the results indicated that the samples were highly hemocompatible in nature indicating the biocompatibility of the scaffolds. Therefore, the scaffolds could be used for the wound-healing application. It is seen by the results that scaffolds with 0.1% copper nanoparticles concentration and 1:1 ratio of chitosan and gelatin possess lowest hemocompatibility, thereby making it the suitable scaffold for the wound-healing application.

In vitro biodegradation study

Degradation occurs usually because of the dissolution of scaffolds that are exposed to PBS. It is very essential, because it allows the cells to form their own extracellular matrix (O'Brien 2011). To determine the scaffold's effect over the cell viability growth here within, Fig. 6 represents in vitro degradation rates of the scaffolds. Figure 6 shows that F1, F2, and F3 are the control scaffolds for the copper doped scaffolds, i.e., F4, F5, and F6, respectively. It is

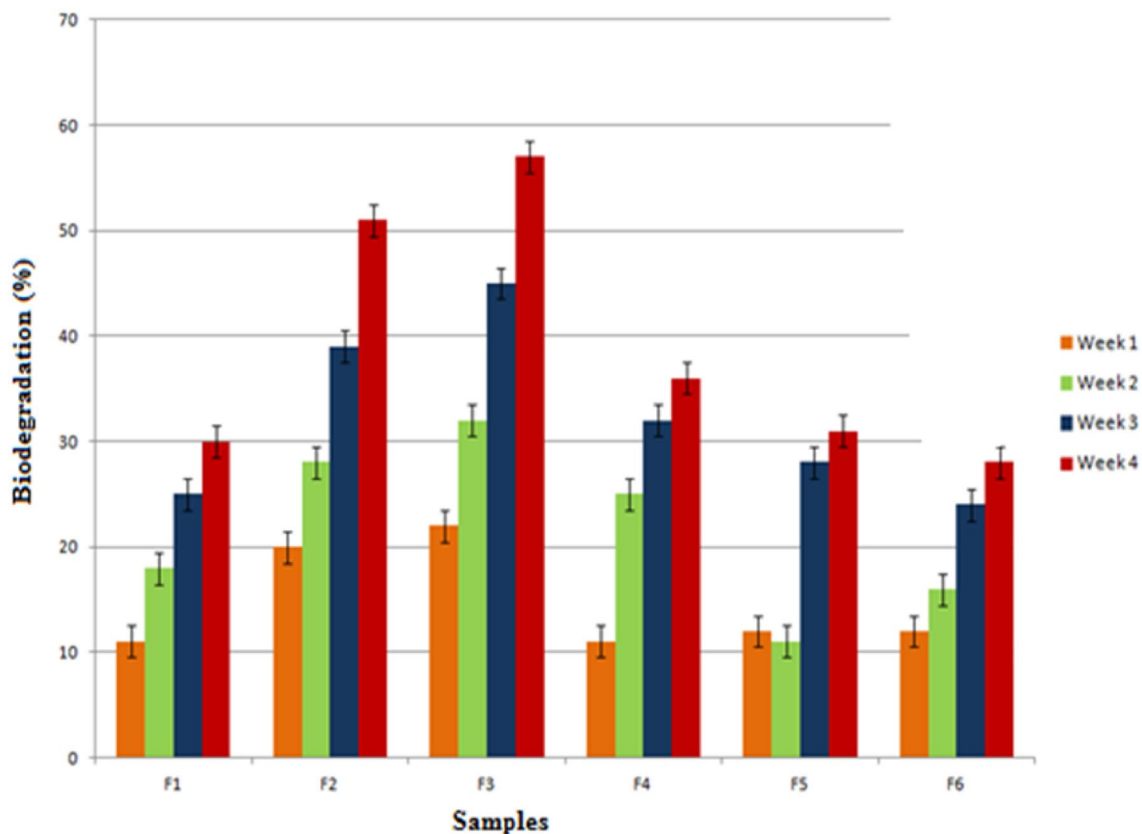


Fig. 6 Biodegradation study of the scaffolds with and without copper nanoparticles in 4 weeks

clearly visible from the plot that, after addition of copper nanoparticles, the degradation rates have lowered to 37% approximately in comparison to the control scaffolds. While, in case of chitosan–gelatin scaffold with 0.2% copper nanoparticles, the scaffolds have shown much lowered rate of biodegradation (15%) in comparison to scaffolds with 0.1%. It is also seen that the control scaffolds F2 and F3 without copper nanoparticles where gelatin concentration is higher show the highest rate of degradation, i.e., 47% with respect to the control scaffold with 1:1 ratio of chitosan and gelatin.

Hence, it can be said that, after the addition of copper nanoparticles, the rate of biodegradation has gradually dropped, thereby making the scaffold best suitable for wound-healing application, as this is going to provide a better strength and stability to the cells (Gurtner et al. 2008).

MTT assay

The MTT assay showed that scaffolds with copper concentration of 0.01% showed higher proliferation rate among all the scaffolds. However, chitosan and gelatin scaffolds with 1:1 ratio also proved to have a better cell proliferation and viability in comparison to the other control scaffolds. At the end of 7th day, also the rate of cell proliferation was higher in case of F4, and therefore, it can be inferred from it that this scaffold shows best-suited characteristics for wound-healing potential. Figure 7 shows the metabolic activity of the cells over the scaffolds.

Afterwards, DCFDA assay was performed to evaluate oxidative stress occurring in the scaffolds due to the presence of copper nanoparticles in Fig. 8a–f where Fig. 8a–c served as control for copper-doped scaffolds in Fig. 8d–f, respectively. It was clearly seen that no fluorescence was

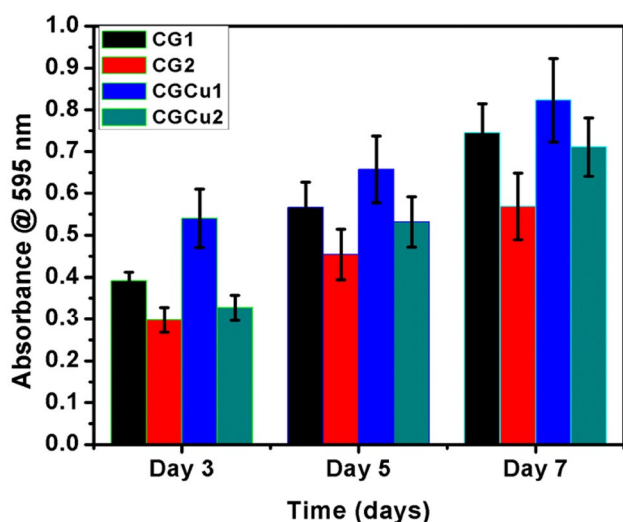


Fig. 7 Proliferation assay of cells on different scaffolds with and without copper nanoparticles after 3, 5, and 7 days of cell seeding

observed in the scaffolds when observed under microscope. There was no oxidative stress occurring within the copper-doped scaffolds. Hence, proving that there was no reactive oxygen species being generated in the scaffolds due to the presence of copper and making them suitable for tissue engineering application.

Microscopic evaluation of cell-seeded scaffolds

Microscopic visualization was done for the cell-seeded scaffolds and the images were taken after 7 day incubation. Microscopy helped to obtain higher resolution optical images in the 3D scaffolds and thereby determined the colonization of skin cells over the scaffold. Live and dead cells were clearly visible in the fluorescence microscopy. As shown in Fig. 8g–l, the presence of live cells in green color has occurred all across the scaffolds. This green color represents the live cells present over the scaffolds after 7 day incubation.

Cell attachment study

The micrographs showed the presence of the cells attached on the scaffold surfaces. Cell growth on the scaffolds was seen in the SEM images after seeding the cells over the control scaffolds and scaffolds having copper nanoparticles. Figure 9 shows the morphological changes in the adherent cells after seeding them into the scaffolds. The analysis was done after, an incubation period of 7 days, the layer of fibroblasts cells can be seen uniformly distributed over the scaffold's surface. In Fig. 9e, f, we can see the layer which has completely filled in the pores of the scaffold, thereby proving the effectiveness of copper nanoparticles in cell growth and proliferation. Figure 9g–i also shows the release study of copper nanoparticles done through the EDAX mapping analysis. In Fig. 9h, i, it was observed that copper releases around 4%, while, in Fig. 9g, no such release was observed as the amount of copper present was lesser. Hence, proving effective release of copper nanoparticles required for proper wound healing.

Conclusion

In the current study, successful development of copper nanoparticle-doped chitosan and gelatin-based scaffolds for skin tissue engineering has been done. It is depicted that, after incorporation of 0.1% copper nanoparticles in the scaffolds, the scaffold turned out to be best suited for skin cell culture. This could be concluded on the basis of mechanical strength imparted by the copper nanoparticles which were synthesized by green-chemical reduction method. The SEM analysis of these scaffold proved that, after addition of

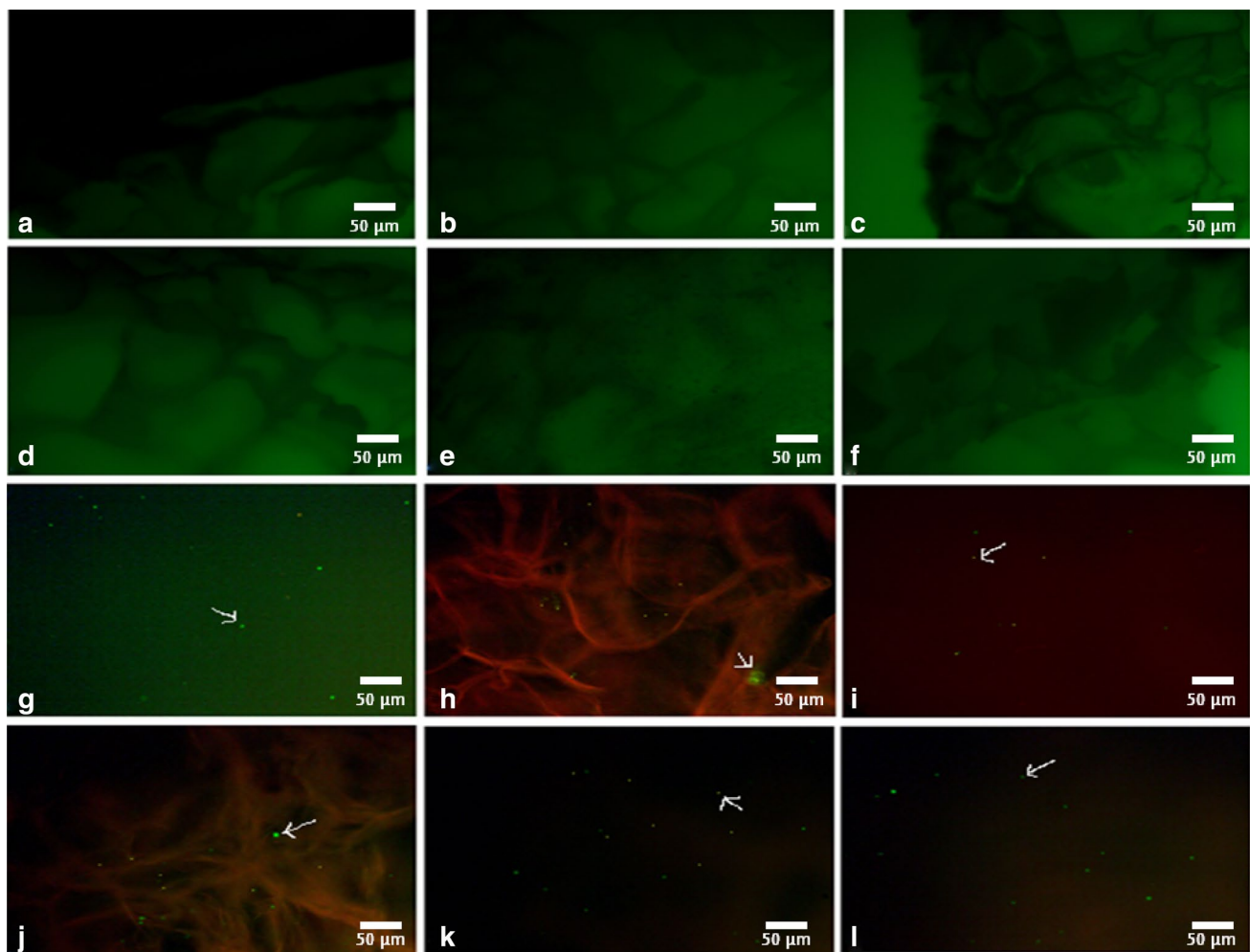


Fig. 8 Microscopic images of cell-seeded scaffolds with and without copper nanoparticles **a** F1, **b** F2, **c** F3, **d** F4, **e** F5, and **f** F6

copper nanoparticles, the pore diameter for cell infiltration was highly influenced. This improved property also resulted in enhanced porosity of scaffold which ultimately showed better results in cell adhesion and proliferation. Improved porosity which was obtained as an outcome of enhanced mechanical stability of the scaffold was also a significant aspect to ensure the proper influx of nutrients and also efflux of the toxic and biodegradable products. Copper nanoparticles were observed not to affect the hemocompatibility of the scaffolds which was done to assess the *in vivo* blood compatibility of scaffold material. In addition, there was no

oxidative stress observed in the cells, in copper-doped scaffolds. Live and dead assay suggested that there was proper growth of cells after 7 day incubation time of the cell-seeded scaffold with copper nanoparticles. There was no leaching of copper nanoparticles in the F4 scaffold, and thus, release of copper nanoparticles was quite slow and effective. The results on the scaffold evaluation suggest that the copper nanoparticle-doped chitosan–gelatin composite scaffold could be a suitable asset for wound-healing application also. *In vivo* studies if conducted further could prove the essentiality of these scaffolds for wound-healing phenomenon.

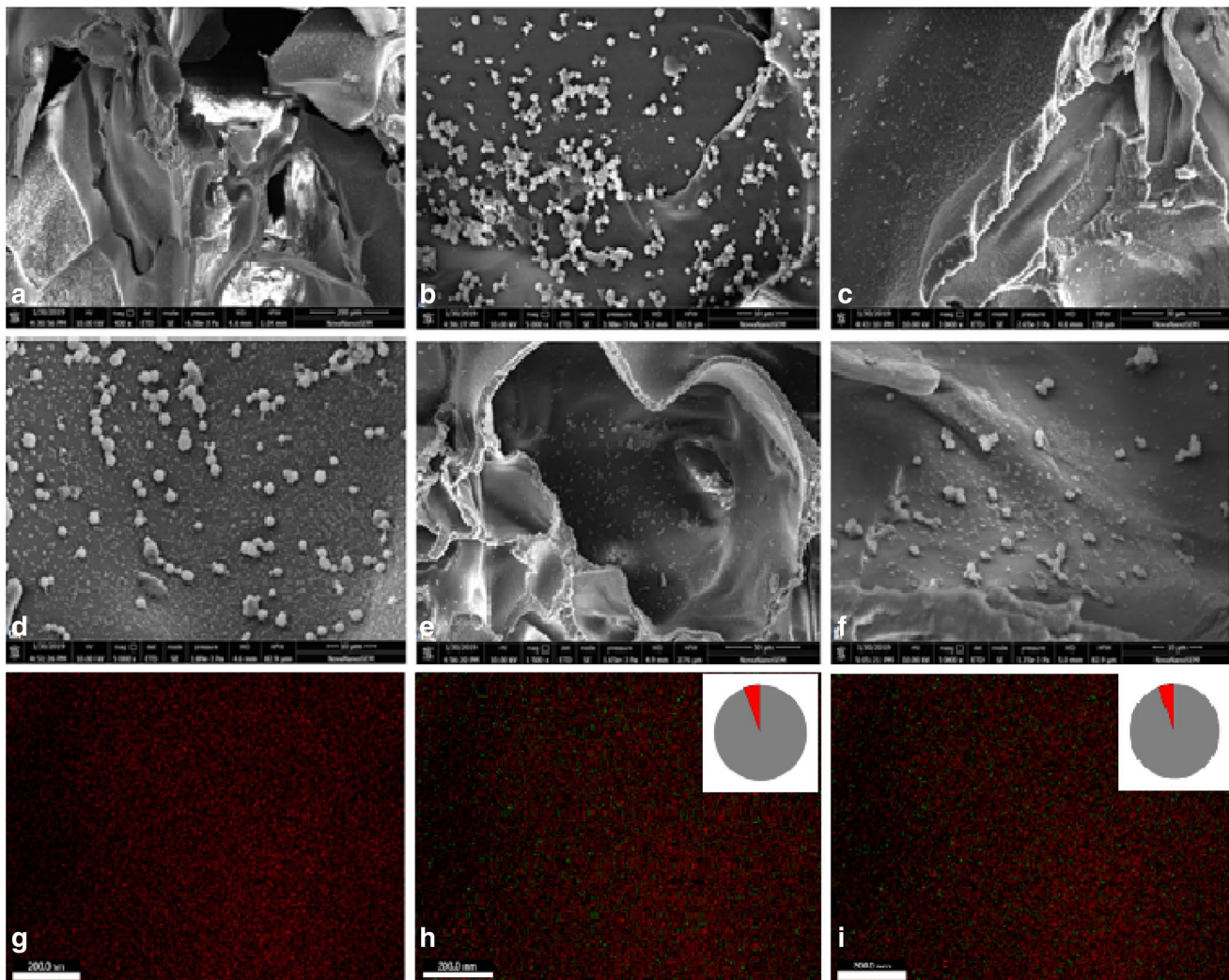


Fig. 9 SEM micrographs of cell-seeded scaffolds with and without copper nanoparticles (a–f), respectively, and EDAX mapping showing copper release in g–i

Acknowledgements This study was supported by the Central Instrument Facility Center (CIFC), IIT (BHU). The authors are also thankful to MHRD for providing fellowship and to IIT BHU for the other infrastructural facility to the first author to carry this work.

Compliance with ethical standards

Conflict of interest The authors declare no competing financial interest.

References

Azad AK et al (2004) Chitosan membrane as a wound-healing dressing: characterization and clinical application. *J Biomed Mater Res Part B Appl Biomater* 69(2):216–222

- Betancourt-Galindo R et al (2014) Synthesis of copper nanoparticles by thermal decomposition and their antimicrobial properties. *J Nanomater* 2014:10
- Borkow G, Okon-Levy N, Gabbay J (2010) Copper oxide impregnated wound dressing: biocidal and safety studies. *Wounds* 22(12):301–310
- Chhabra H et al (2016) A nano zinc oxide doped electrospun scaffold improves wound healing in a rodent model. *RSC Adv* 6(2):1428–1439
- D’Mello S et al (2015) Incorporation of copper into chitosan scaffolds promotes bone regeneration in rat calvarial defects. *J Biomed Mater Res Part B Appl Biomater* 103(5):1044–1049
- Gérard C et al (2010) The stimulation of angiogenesis and collagen deposition by copper. *Biomaterials* 31(5):824–831
- Gopal A et al (2014) Chitosan-based copper nanocomposite accelerates healing in excision wound model in rats. *Eur J Pharmacol* 731:8–19
- Guan J et al (2005) Preparation and characterization of highly porous, biodegradable polyurethane scaffolds for soft tissue applications. *Biomaterials* 26(18):3961–3971

- Gurtner GC et al (2008) Wound repair and regeneration. *Nature* 453(7193):314
- Hilmi ABM et al (2013) In vitro characterization of a chitosan skin regenerating template as a scaffold for cells cultivation. *Springerplus* 2(1):79
- Hu Gf (1998) Copper stimulates proliferation of human endothelial cells under culture. *J Cell Biochem* 69(3):326–335
- Karp JM, Dalton PD, Shoichet MS (2003) Scaffolds for tissue engineering. *MRS Bull* 28(4):301–306
- Kaur T, Thirugnanam A (2016) Tailoring in vitro biological and mechanical properties of polyvinyl alcohol reinforced with threshold carbon nanotube concentration for improved cellular response. *RSC Adv* 6(46):39982–39992
- Khan A et al (2016) A chemical reduction approach to the synthesis of copper nanoparticles. *Int Nano Lett* 6(1):21–26
- Kummrow A et al (2013) Quantitative assessment of cell viability based on flow cytometry and microscopy. *Cytom Part A* 83(2):197–204
- Lee Y et al (2012) Reduction of inflammatory responses and enhancement of extracellular matrix formation by vanillin-incorporated poly (lactic-co-glycolic acid) scaffolds. *Tissue Eng Part A* 18(19–20):1967–1978
- Liusuwan RA et al (2008) Impaired healing because of copper deficiency in a pediatric burn patient: a case report. *J Trauma Acute Care Surg* 65(2):464–466
- Martin F et al (2005) Copper-dependent activation of hypoxia-inducible factor (HIF)-1: implications for ceruloplasmin regulation. *Blood* 105(12):4613–4619
- Moore P, rapid A (1990) pH insensitive, two color fluorescence viability (cytotoxicity) assay. *J Cell Biol* 111:58a
- O'brien FJ (2011) Biomaterials & scaffolds for tissue engineering. *Mater Today* 14(3):88–95
- Peter M et al (2010) Novel biodegradable chitosan–gelatin/nano-bioactive glass ceramic composite scaffolds for alveolar bone tissue engineering. *Chem Eng J* 158(2):353–361
- Sarkar SD et al (2013) Chitosan–collagen scaffolds with nano/micro-fibrous architecture for skin tissue engineering. *J Biomed Mater Res Part A* 101(12):3482–3492
- Sen CK et al (2002) Copper-induced vascular endothelial growth factor expression and wound healing. *Am J Physiol Heart Circ Physiol* 282(5):H1821–H1827
- Ueno H, Mori T, Fujinaga T (2001) Topical formulations and wound healing applications of chitosan. *Adv Drug Deliv Rev* 52(2):105–115
- Xu J et al (2012) Mechanical enhancement of nanofibrous scaffolds through polyelectrolyte complexation. *Nanotechnology* 24(2):025701
- Yang S et al (2001) The design of scaffolds for use in tissue engineering. Part I. Traditional factors. *Tissue Eng* 7(6):679–689
- Yannas I et al (1989) Synthesis and characterization of a model extracellular matrix that induces partial regeneration of adult mammalian skin. *Proc Natl Acad Sci* 86(3):933–937
- Yildirimer L, Thanh NT, Seifalian AM (2012) Skin regeneration scaffolds: a multimodal bottom-up approach. *Trends Biotechnol* 30(12):638–648
- Zhuang C, Tao F, Cui Y (2015) Anti-degradation gelatin films crosslinked by active ester based on cellulose. *RSC Adv* 5(64):52183–52193
- Zinc C, Levels ST, Mirastschijski U, Martin A, Jorgensen LN, Sampson B, Magnus S (2013) *Ågren Biol Trace Elem Res* 153:76–83